Turbulent Boundary Layer on a Smooth Flat Plate With and Without Heat Transfer," *Journal of Fluid Mechanics*, Vol. 18, Pt. 1, Jan. 1964, pp. 117–143.

[11] Reshotko, E. and Tucker, M., "Approximate Calculation of the Compressible Turbulent Boundary Layer With Heat Transfer and Arbitrary Pressure Gradient," TN 4154, 1957, NACA.

[12] Dhawan, S. and Narasimha, R., "Some Properties of Boundary Layer Flow During the Transition From Laminar to Turbulent Motion," *Journal of Fluid Mechanics*, Vol. 3, No. 4, April 1958, pp. 418–436.

[13] Maslen, S. H., "Inviscid Hypersonic Flow Past Smooth Symmetric Bodies," *AIAA Journal*, Vol. 2, No. 6, June, 1964, pp. 1055–1061.

[14] Maslen, S. H., "Asymmetric Hypersonic Flow," CR-2123, Sept. 1972, NASA.

[15] DeJarnette, F. R., "Calculation of Heat Transfer on Shuttle-Type Configurations Including the Effects of Variable Entropy at Boundary Layer Edge," CR-112180, Oct. 1972, NASA.

[16] Hopkins, E. J. and Inouye, M., "An Evaluation of Theories for Predicting Turbulent Skin Friction and Heat Transfer on Flat Plates at Supersonic and Hypersonic Mach Numbers," *AIAA Journal*, Vol. 9, No. 6, June, 1971, pp. 993–1003.

[17] Cleary, J. W., "Effects of Angle of Attack and Bluntness on Laminar Heating-Rate Distributions of a 15° Cone at a Mach Number of 10.6," TN D-5450, 1969, NASA.

[18] Hillsamer, M. E., and Rhudy, J. P., "Heat-Transfer and Shadowgraph Tests of Several Elliptical Lifting Bodies at Mach 10," U.S. Air Force, AEDC-TDR-64-19, 1964, Arnold Engineering Development Center, Tullahoma, Tenn.

JANUARY 1975 J. SPACECRAFT VOL. 12, NO. 1

High Angle-of-Attack Aerodynamics on a Slender Body with a Jet Plume

R. C. NELSON* AND E. L. FLEEMAN†
Air Force Flight Dynamics Laboratory, Wright-Patterson Air Force Base, Ohio

This paper presents an aerodynamic analysis of data obtained from recent wind-tunnel tests on a slender body configuration. Force and moment coefficients are presented for angles of attack up to 180°, Mach numbers up to 2.2, and Reynolds numbers (based on diameter) up to 10^6. The rocket exhaust plume was simulated by exhausting cold air (ambient total temperature) through the nozzle of the model. This permitted study of the plume interference effects on the aerodynamic coefficients. The jet effects on normal force were found to be important when the angle of attack exceeded 40° in subsonic flow and 90° in supersonic flow. Deflecting the nozzle at high angles of attack also caused large excursions in the center-of-pressure location. Another problem associated with high angle-of-attack flight is the appearance of large side forces and yawing moments for a symmetric flight condition. These are due to steady asymmetric shedding of the body vortices. Data are presented which illustrate the influence of Mach number and Reynolds number on the out-of-plane forces.

Nomenclature

A = cross-sectional area of cylindrical portion of the body
A_b = body base area
A_p = planform area
C_{d_n} = cross-flow drag coefficient of cylinder, $F_n/(q_n \Delta l_{cy} d)$
C_m = pitching moment coefficient, $M/(qAd)$ (positive nose up)
C_n = yawing moment coefficient, $N/(qAd)$ (positive nose to the right)
C_N = normal force coefficient, $F_n/(qA)$
C_Y = side force coefficient, $Y/(qA)$
ΔC_N = $C_{N\,\text{jet on}} - C_{N\,\text{jet off}}$
d = model diameter or circular cylinder diameter
d_{NT} = nose tip diameter
F_n = normal force
l = body length
l_{cy} = cylinder length
l_N = nose length
M = pitching moment or Mach number
N = yawing moment
P_{t_j} = total pressure of the jet
P_{t_∞} = total pressure of the freestream
q = dynamic pressure
q_n = cross-flow dynamic pressure
R_{e_d} = Reynolds number based on model diameter
U = free-stream velocity
X_{cp} = location of center-of-pressure from the model nose
X_{cg} = location of center-of-gravity from model nose, 8.4d
Y = side force
α = angle-of-attack
β = angle-of-sideslip
δ = nozzle deflection (positive deflection into the wind)
η = cross-flow drag proportionality factor

Presented as Paper 74–110 at the AIAA 12th Aerospace Sciences Meeting, Washington, D.C., January 30–February 1, 1974; submitted February 21, 1974; revision received August 2, 1974. The authors gratefully acknowledge assistance by J. Jones (ARO, Inc.), D. Shereda (AFFDL), D. Perper (Hughes Aircraft), J. Donahoe (Martin Orlando), and E. Chambers (Raytheon Missile Systems Division) for efforts in supporting schlieren photography, computer calculations, and model and balance construction.

Index category: Missile Aerodynamics.

* Aerospace Engineer, Control Criteria Branch, Flight Control Division. Member AIAA.

† Aerospace Engineer, Control Criteria Branch, Flight Control Division. Member AIAA.

Introduction

IN recent years tactical aircraft and missiles have been designed with increased emphasis on achieving more maneuverability. As a result of this design trend, aircraft and missiles are flying at much higher angles of attack than in the past. In fact, there are designs presently under consideration for missiles which will fly at angles of attack ranging from 0°–180°. The design of such highly maneuverable missiles has prompted a renewed interest

in the aerodynamics of slender body configurations at high angles of attack.

One means of achieving increased maneuverability is by use of a thrust-vector-control system. Although there is a limited amount of experimental data available on slender missile configurations at large angles of attack, data on the influence of a rocket exhaust plume over the high angle of attack range are almost nonexistent.

This paper summarizes a comprehensive wind tunnel investigation of a slender body at high angles of attack. The effects of Mach number, Reynolds number and jet-plume interference on the aerodynamic coefficients are presented.

Description of Test Facilities and Models

Test Facilities

The aerodynamic data presented in the paper were obtained from wind tunnel tests conducted at the Arnold Engineering Development Center (AEDC). Two geometrically similar models were tested in four different tunnels. The smaller model was tested in the Von Kármán Facility (VKF) Tunnel A and the Propulsion Wind Tunnel (PWT) 4T, while the larger model was tested in the PWT 16T and 16S. These tunnels are of the closed circuit continuous-flow type which varies Reynolds number by increasing total pressure for a constant total temperature of 90°–150°F. VKF Tunnel A has a 40 × 40 in. test section and is capable of operating at Mach numbers from 1.5 to 6. The PWT-4T tunnel has a 4 × 4 ft test section with a Mach number range from 0.1 to 1.3. The PWT-16T has a 16 × 16 ft test section and a Mach number range from 0.2 to 1.6. The PWT-16S also has a 16 × 16 ft test section but the Mach number range is 1.2 to 4.6. A detailed description of the tunnels is included in the "AEDC Test Facilities Handbook."[1]

Various sting, strut, and mounting supports were required to traverse the 180° angle-of-attack regime. Figure 1 shows photographs of the models and two of the support assemblies which were used. The jet-plume was simulated by pumping cold air through the support system into the model and then exhausting the air through the model nozzle.

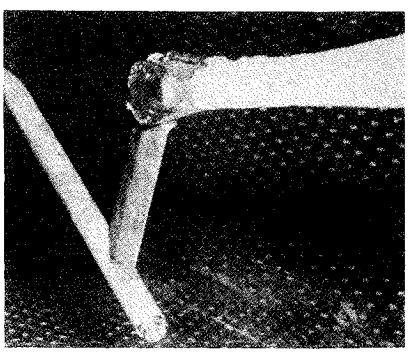

a)

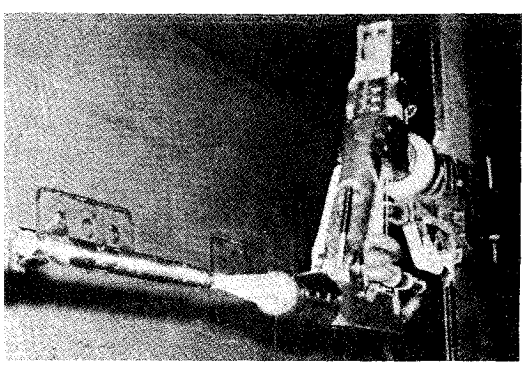

b)

Fig. 1 Model and support assemblies. a) Side strut support for Model 1 in AEDC Tunnel 4T. b) Nose sting support for Model 2 in AEDC 16S.

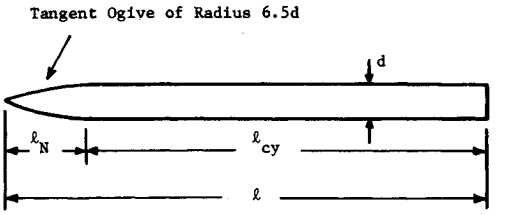

Geometry	Model 1	Model 2
d	1.375 inches	3.667 inches
ℓ/d	14.83	14.55
ℓ_N/d	2.42	2.5
d_{NT}/d	0.091	0 (Sharp)

Fig. 2 Sketch of model.

Models

A representative sketch of the models used during the tests is shown in Fig. 2. The models consist of a tangent ogive nose of fineness ratio of approximately 2.5 and a cylindrical afterbody of fineness ratio of approximately 12. The models are similar except for differences in nose bluntness ratio and a small difference in model fineness ratio. Model 1 has a nose bluntness ratio of 9%, whereas model 2 has essentially a sharp nose; that is, 0% bluntness. Both models were designed so that the jet forces and moments were nonmetric (not measured). Thus the plume interference effects on the aerodynamic coefficients could be easily measured.

Each model was equipped with a conical nozzle which could be deflected ±15° from the model centerline. In addition to the main jet simulation, the larger model has four small nozzles located near the nose in order to simulate a reaction roll control system. Table 1 gives the geometric and aerodynamic characteristics of the roll and main jet nozzles.

Table 1 Jet characteristics

	Model 1	Model 2	
Characteristic	Main jet	Main jet	Roll jet
Nozzle Exit Mach No.	3.14	3.77	3.56
Nozzle Exit Diam. (in.)	0.895	3.196	0.285
Nozzle Throat Diam. (in.)	0.406	1.083	0.117
Exit Angle (deg.)	15.0	15.4	22.0
Distance from Nose to Exit (in.)	20.897	56.000	15.866
Distance from Model Centerline to Jet Centerline (in.)	0	0	1.459
Number of Jets	1	1	4

Aerodynamic Analysis

This section presents the normal force coefficient and center-of-pressure location for the model configurations. Both models were tested over an angle-of-attack range from 0° to 180°. Other parameters which were varied include Mach number, Reynolds number, main jet pressure ratio, main jet deflection, and roll jet conditions.

Mach Number and Model Support Effects

Figure 3 illustrates the influence of Mach number on the normal force coefficient C_N for high angles of attack. For Mach

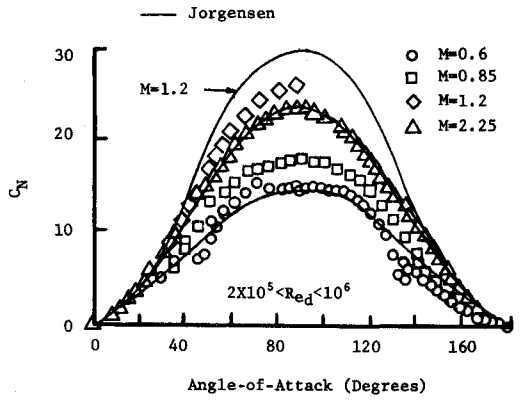

Fig. 3 Effect of Mach number on normal force coefficient.

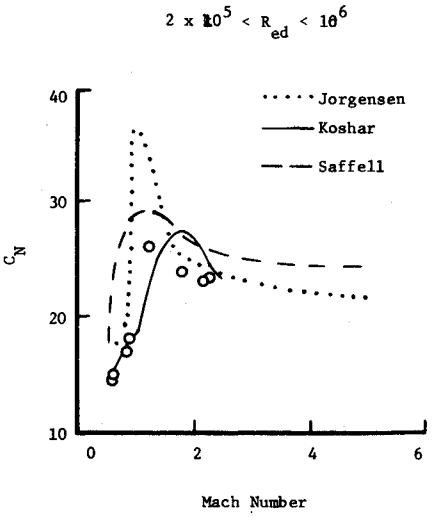

Fig. 5 Comparison of normal force with theory for 90° angle of attack.

numbers of 0.6 and 0.85, the C_N curve flattens as the angle of attack approaches 90°. This characteristic has been observed in the past. Recently Jorgensen[2] was able to predict this trend in the C_N curve based upon the following formula:

$$C_N = (A_b/A) \sin 2\alpha' \cos(\alpha'/2) + \eta C_{d_n} (A_p/A) \sin^2 \alpha' \qquad (1)$$

where $\alpha' = \alpha$ for $0° \leqq \alpha \leqq 90°$ and $\alpha' = 180° - \alpha$ for $90° \leqq \alpha \leqq 180°$. The first term in Eq. (1) is the familiar slender body result and the second term is the viscous cross-flow contribution. Jorgensen attributed the flattening of the C_N curve to the strong Reynolds number influence on the cross-flow drag coefficient C_{d_n}. Returning to Fig. 3, note that the peak C_N increases with Mach number up to Mach 1.2 and then decreases for Mach 2.25. This effect can again be traced to the cross-flow drag coefficient. The cross-flow drag coefficient increases with Mach number up to approximately Mach 1, whereupon C_{d_n} decreases with increasing cross-flow Mach number. Thus one would expect to have the peak C_N near Mach 1.

The center-of-pressure location measured in calibers from the nose is shown in Figure 4. The X_{cp}/d appears to increase linearly over the range of angle of attack from approximately 15° to 160°. Below approximately 15° and above 160° the center-of-pressure is seen to shift rapidly. For the low angles of attack the X_{cp}/d is near the nose, and for the extreme angles of attack it moves toward the base of the model.

Support interference is considered to have a small effect on data accuracy. The mismatch in C_N and X_{cp}/d at overlapping angles of attack for the aft sting, side strut, and nose sting supports is small, indicating negligible support interference.

Comparison with Aerodynamic Prediction Methods

Several techniques for estimating the aerodynamic coefficients were compared with the data. In particular the methods developed in Refs. 2–4 were used. Jorgensen's[2] methods for computing the static aerodynamic coefficients are an extension of Allen's cross-flow theory to higher angles of attack. Saffell et al.[3] and Koshar et al.[4] also modified various well-known slender body and cross-flow theories to the higher angle of attack region.

Figure 5 compares predictions of C_N with experimental data for an angle of attack of 90° and a Mach number range from 0.85–2.2. The methods all over predict the values of C_N, particularly at the transonic Mach numbers. The best agreement with the measured C_N is given by Jorgensen's method. All of the methods showed good agreement with the data for X_{cp}/d.

Figure 6 compares predictions of C_N with experimental data for an angle of attack of 40° and a Reynolds number range of 10^5 to 7×10^5. The normal force coefficient tends to decrease in magnitude as the Reynolds number is increased, and is consistent with the trend predicted by Jorgensen. Conditions where there is a strong dependency of normal force coefficient on Reynolds number occur for low cross-flow Mach number (less than 0.6) with high cross-flow Reynolds number (greater than 2×10^5). There was a negligible effect of Reynolds number on C_N for the supersonic Mach numbers investigated. The center-of-pressure location was found to be relatively constant with changes in Reynolds number.

Jet Effects

As mentioned previously the effect of the rocket exhaust-plume was simulated by exhausting cold air (ambient total temperature)

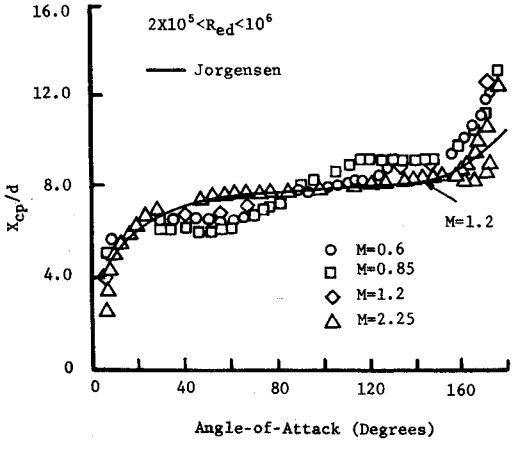

Fig. 4 Effect of Mach number on X_{cp}/d.

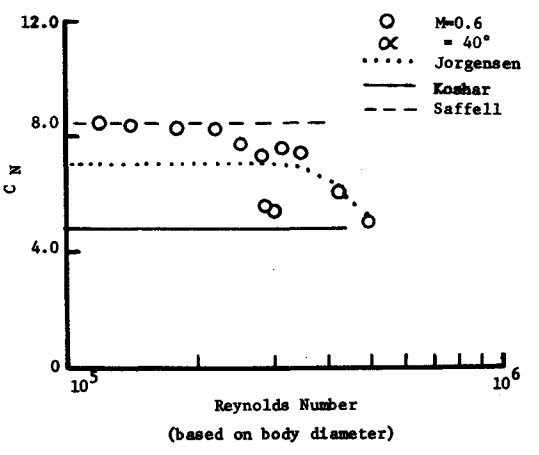

Fig. 6 Effect of Reynolds number on normal force coefficient.

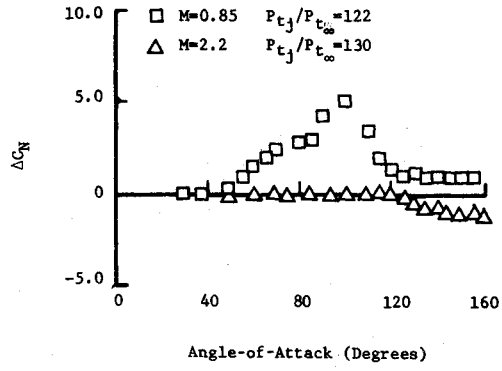

Fig. 7 Effect of main jet on normal force coefficient.

through the model nozzle. Figure 7 illustrates the effect of the main jet on C_N from 30°–160° angle of attack. Notice that the main jet increases C_N for the subsonic freestream Mach number in the 40°–120° region. However, in the supersonic case the main jet results show a small decrease in C_N for angles of attack greater than 120°. There was no noticeable influence observed of jet pressure on the center-of-pressure location over this angle-of-attack range.

Deflection of the main jet for a supersonic freestream Mach number has a negligible effect on normal force coefficient except at extreme angles of attack. For angles of attack greater than 140°, deflecting the jet into the wind results in a relatively small decrease in C_N. A negative nozzle deflection (away from the wind) results in a correspondingly small increase in C_N. But there is a large effect of nozzle deflection on the center-of-pressure location. This is illustrated in Fig. 8 for a freestream Mach number of 2.2. Although center-of-pressure location is not affected by nozzle deflection for the supersonic freestream Mach number and angles of attack less than 140°, positive nozzle deflection at large angles of attack results in an X_{cp}/d shift toward the nose. This occurs because the aft portion of the model is shielded from the free-stream by the jet. The X_{cp}/d shift is nearly 4 calibers for the 15° nozzle deflection at 160° angle of attack. A nozzle deflection of $-15°$ does not significantly alter the X_{cp}/d location from the undeflected results.

As indicated earlier, Model 2 was tested with roll control jets located near the nose and used the same cold air supply as the main jet. Roll jets were tested at a variety of jet pressures and modes of operation (jets off, left roll, right roll, all four roll jets on). Analysis of the data indicates that the roll jets produced little or no change in aerodynamics.

Out-of-Plane Forces and Moments

Another interesting problem associated with high angle-of-attack flight is the occurrence of substantial out-of-plane forces and moments on a slender body at zero angle of sideslip ($\beta = 0$). These forces and moments have been traced to the asymmetric

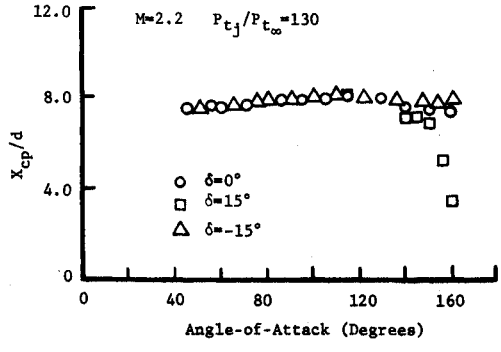

Fig. 8 Effect of nozzle deflection on center-of-pressure location.

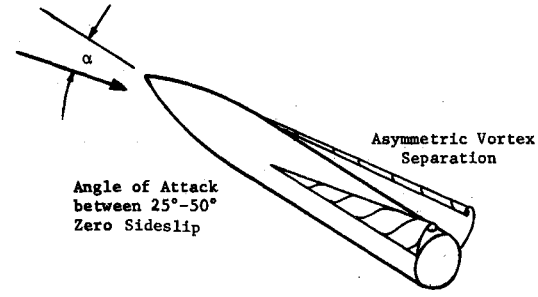

Fig. 9 Asymmetric flow separation.

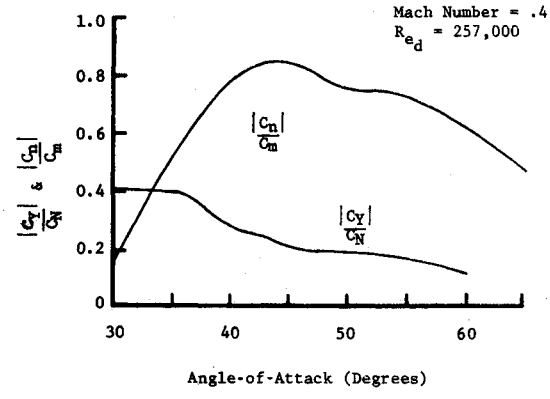

Fig. 10 Relative magnitude of out-of-plane forces and moments.

shedding of the body vortices as shown in Fig. 9. Various experimental investigations [5–8] have been conducted to gain a better understanding of the flow around a slender body at high angles of attack as well as determining the factors influencing the magnitude of the out-of-plane forces and moments.

Figure 10 shows the relative magnitude of the out-of-plane forces and moments with respect to the normal force and pitching moment coefficients. Here we see that the side force is approximately 40% of the normal force in the vicinity of $\alpha = 30°$ and then decreases with increasing angle of attack. A similar result was presented by Krouse.[7] On the other hand, the yawing moment observed in this investigation reaches a maximum of

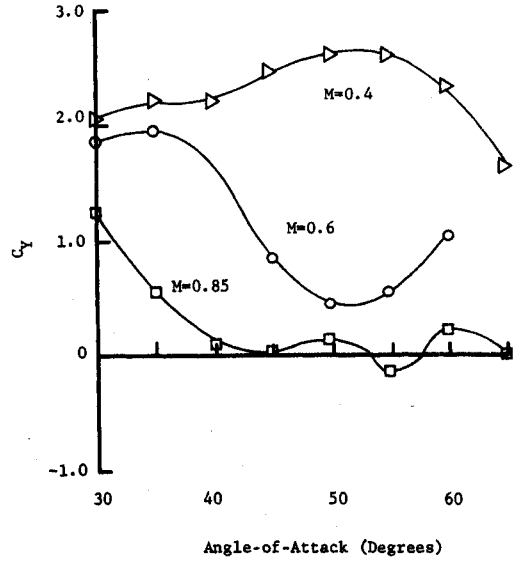

Fig. 11 Effect of Mach number on induced side force coefficient.

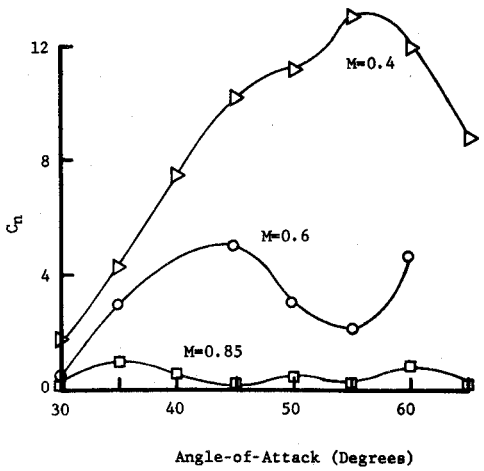

Fig. 12 Effect of Mach number on induced yawing moment coefficient.

approximately 85% of the pitching moment in the vicinity of $\alpha = 45°$.

Figures 11 and 12 show the influence of the freestream Mach number on the side force and yawing moment coefficients. As the Mach number is increased, both the side force and yawing moment coefficients decrease. This trend is similar to that found by Pick.[8] Results such as those presented in Figs. 11 and 12 as well as from other investigations have given the impression that the out of plane forces can only occur in the subsonic region. However, Fig. 13 indicates the presence of a yawing moment at a Mach number of 1.76. Unfortunately this particular test was conducted primarily to obtain low angle-of-attack data. Therefore only a limited amount of data was obtained over the angle-of-attack range for which asymmetric vortex shedding would occur.

The out-of-plane forces and moments were found to be sensitive to Reynolds number. Figure 14 illustrates the Reynolds number effect on the side force coefficient for a fixed angle of attack of 40°. Although the data exhibit considerable scatter, the side force coefficient increases with Reynolds number up to approximately 250,000. Further increases in Reynolds number result in lower values of the side force coefficient. A similar result was observed for the yawing moment coefficient.

There are many factors influencing the magnitude of the out-of-plane forces and moments; therefore, the reader should interpret the results of this section only as qualitative information on the influence of Mach and Reynolds numbers.

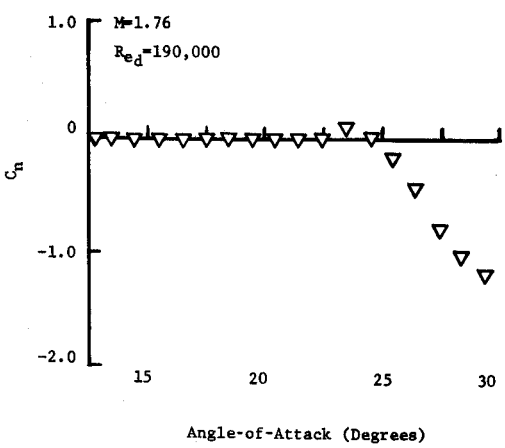

Fig. 13 Induced yawing moment coefficient for $M = 1.76$.

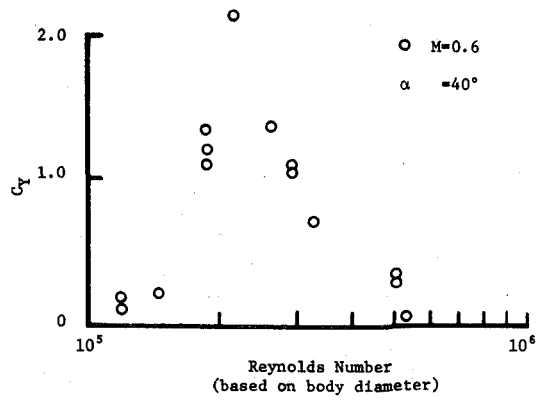

Fig. 14 Effect of Reynolds number on induced side force coefficient.

Conclusions

The following conclusions were reached in this study.

1) The theoretical estimates of C_N and X_{cp}/d were found to be consistent with the trends of the experimental data. Jorgensen's prediction method had the best correlation with the data.

2) There is a strong Reynolds number effect on C_N for Mach numbers less than one and angle of attack near 90° ($C_{N_{max}}$).

3) The aerodynamic interference effects induced by an undeflected main jet was found to be relatively small compared to the jet-off conditions. The roll jet produced little or no change in the aerodynamic coefficients.

4) Deflecting the main jet into the supersonic freestream at high angles of attack causes a large shift in the center of pressure.

5) The out-of-plane forces and moments associated with the asymmetric shedding of the body vortices decrease in magnitude as the Mach number approaches unity. However, at supersonic Mach numbers out-of-plane forces and moments can reappear. In addition, the out-of-plane forces and moments were found to vary significantly with Reynolds number. The peak values of the forces and moments occurred for cross-flow Reynolds numbers between 140,000 and 230,000.

References

[1] "Test Facilities Handbook," 8th ed., Dec. 1969, Arnold Engineering Development Center, Tullahoma, Tenn.

[2] Jorgensen, L. H., "Prediction of Static Aerodynamic Characteristics for Space-Shuttle-Like and Other Bodies at Angles of Attack from 0° to 180°," TN D-6996, Jan. 1973, NASA.

[3] Saffell, B. F., Howard, M. L., and Brooks, E. N., "A Method for Predicting the Static Aerodynamics of Typical Missile Configurations for Angles of Attack to 180 Degrees," NSRDC Rept. 3645, March 1971, Naval Ship Research and Development Center, Bethesda, Md.

[4] Koshar, M. M., Cobb, E. R., et al., "Missile Synthesis and Performance Computer Program," Martin Marietta Computer Manual, July 1971, Martin Marietta Corp., Orlando, Fl.

[5] Thomson, K. D. and Morrison, D. F., "The Spacing, Position and Strength of Vortices in the Wake of Slender Cylindrical Bodies at Large Incidence," *Journal of Fluid Mechanics*, Vol. 50, Pt. 4, 1971 pp. 751–783.

[6] Clark, W. H., Peoples, J. R., and Briggs, M. M., "Occurrence and Inhibition of Large Yawing Moments During High-Incidence Flight of Slender Missile Configurations," *Journal of Spacecraft and Rockets*, Vol. 10, No. 8, Aug. 1973, pp. 510–519.

[7] Krouse, J. R., "Induced Side Forces on Slender Bodies at High Angles of Attack and Mach Numbers of 0.55 and 0.80," NSRDC Test Rept. AL-79, May 1971, Naval Ship Research and Development Center, Bethesda, Md.

[8] Pick, G. S., "Side Forces on Ogive Cylinder Bodies at High Angles of Attack in Transonic Flow," *Journal of Spacecraft and Rockets*, Vol. 9, No. 6, June 1972, pp. 389–390.